



# Measurement of ultrafast optical Kerr effect of Ge–Sb–Se chalcogenide slab waveguides by the beam self-trapping technique



Tintu Kuriakose<sup>a,\*</sup>, Emeline Baudet<sup>b</sup>, Tomáš Halenkovič<sup>c</sup>, Mahmoud M.R. Elsayw<sup>d</sup>, Petr Němec<sup>c</sup>, Virginie Nazabal<sup>b,c</sup>, Gilles Renversez<sup>d</sup>, Mathieu Chauvet<sup>a</sup>

<sup>a</sup> Department of Optics, FEMTO-ST Institute, UMR CNRS 6174, Université Bourgogne Franche-Comté, 15B avenue des Montboucons, 25030 Besançon, France

<sup>b</sup> Equipe Verres et Céramiques-Institut des sciences chimiques de Rennes (ISCR), UMR 6226 Université de Rennes 1-CNRS, Campus de Beaulieu, 35042 Rennes Cedex, France

<sup>c</sup> Department of Graphic Arts and Photophysics, Faculty of Chemical Technology, University of Pardubice, 53210 Pardubice, Czech Republic

<sup>d</sup> Aix Marseille Univ, CNRS, Centrale Marseille, Institut Fresnel, Marseille, France

## ARTICLE INFO

### Keywords:

Ultrafast nonlinear optics  
Nonlinear optical materials  
Slab waveguides  
Kerr effect  
Spatial solitons

## ABSTRACT

We present a reliable and original experimental technique based on the analysis of beam self-trapping to measure ultrafast optical nonlinearities in planar waveguides. The technique is applied to the characterization of Ge–Sb–Se chalcogenide films that allow Kerr induced self-focusing and soliton formation. Linear and nonlinear optical constants of three different chalcogenide waveguides are studied at 1200 and 1550 nm in femtosecond regime. Waveguide propagation loss and two photon absorption coefficients are determined by transmission analysis. Beam broadening and narrowing results are compared with simulations of the nonlinear Schrödinger equation solved by BPM method to deduce the Kerr  $n_2$  coefficients. Kerr optical nonlinearities obtained by our original technique compare favorably with the values obtained by Z-scan technique. Nonlinear refractive index as high as  $(69 \pm 11) \times 10^{-18} \text{ m}^2/\text{W}$  is measured in  $\text{Ge}_{12.5}\text{Sb}_{25}\text{Se}_{62.5}$  at 1200 nm with low nonlinear absorption and low propagation losses which reveals the great characteristics of our waveguides for ultrafast all optical switching and integrated photonic devices.

© 2017 Elsevier B.V. All rights reserved.

## 1. Introduction

The characterization of nonlinear optical properties has an important role in modern photonic functionalities. Different techniques have been employed to determine the third order nonlinear optical constants of bulk/film samples including self-phase modulation (SPM) [1], Mach–Zehnder technique (MZT) [2], degenerate four wave mixing (DFWM) [3], two-photon absorption spectroscopy [4], optical Kerr gate [5], and Z-scan [6,7]. The latter technique is the most widely used one and is appropriate to characterize both bulk material and thin films. The Z-scan is suitable to determine both the real and imaginary part of the nonlinear refractive index. This method is based on the analysis of the diffraction modification due to nonlinear effect of a beam focused in the sample under study while the sample is moved longitudinally. For accurate measurements, it requires samples with very good homogeneity. In addition, this technique cannot be used in very thin layers since the induced beam change becomes indiscernible. Moreover, the thin film under test is often deposited on a substrate

that can perturb or prevent the measurement. Unlike Z-scan, a single laser shot is enough in MZT technique to measure the nonlinearity. Nevertheless, the complex experimental setup based on the pump-probe experiment of the Mach–Zehnder interferometer can be cumbersome. Many techniques have also been developed to analyze nonlinearities in 2-D waveguides. For instance, the SPM technique, which is based on the analysis of the spectral broadening of a beam as a function of intensity, allows  $n_2$  measurements of 2-D waveguides. Likewise, DFWM technique is also well suited to analyze third order susceptibility tensor of 2-D waveguides but it requires injection of synchronized pulses at different wavelengths. Principally, none of these techniques is well suited to study nonlinear properties in very thin layers that form planar waveguides. In this paper, we propose a technique that is convenient to determine the Kerr effect in such structures. The method is based on the direct analysis of the influence of the non-linear effect on the spatial light distribution of a beam propagating in the slab waveguide. The proposed method has several merits. The experimental setup is simple and one laser shot

\* Corresponding author.

E-mail address: [tintu.kuriakose@femto-st.fr](mailto:tintu.kuriakose@femto-st.fr) (T. Kuriakose).

could be sufficient to deduce the Kerr coefficient. The sensitivity is very good especially when self-trapping leads to the formation of spatial soliton. The method can be used even in multimode waveguides and is relatively immune to perturbations due to the substrate. In addition, the proposed technique can be applied to characterize any materials that are deposited under thin films.

Moreover, identifying optical materials for ultrafast all-optical signal processing and more generally nonlinear photonic devices fabrication [8] have attracted researcher's attention over the past decades. Key materials such as silicon [9] or III–V compounds [10,11] have been investigated. Although excellent results have been obtained for given spectral range, the quest for better material with stronger Kerr coefficient, lower two-photon absorption (TPA), negligible free carrier absorption and low-cost processing techniques are still relevant. Chalcogenide glasses that have large Kerr nonlinearity, ultrafast response time, and optical transmittance in the infrared are among the materials that could fulfill part of these requirements. While few chalcogenide compositions and systems such as  $\text{As}_2\text{S}_3$  [3],  $\text{As}_2\text{Se}_3$  [12],  $\text{Ge-As-S(Se)}$  [13], and  $\text{Ge-Sb-S}$  [14,15] have been intensely explored for nonlinear optical properties purposes, new chalcogenide glasses are still synthesized, with the hope that a high-bit-rate optical processing system operating at low peak power can be reached. In the present work, the proposed characterization technique is applied to  $\text{Ge-Sb-Se}$  sputtered thin films. These sputtered films are of interest due to their low phonon energy, large glass forming region, excellent IR transmittance, and lower toxicity in comparison with arsenic based glasses. Moreover, the presence of antimony could reduce the detrimental photosensitivity of the material [16]. Recently, the linear and nonlinear optical properties of  $\text{Ge-Sb-Se}$  glasses have been studied at near and mid infrared wavelengths [17–21]. Krogstad et al. reported nonlinear properties of bulk and single mode strip waveguides made of  $\text{Ge}_{28}\text{Sb}_{12}\text{Se}_{60}$  glass at a wavelength of 1030 nm [22]. Nevertheless, the Kerr nonlinear response of  $\text{Ge-Sb-Se}$  amorphous materials, when fabricated in thin film forms, needs further studies. The characterization technique we propose is based on the analysis of beam self-action and more specifically on beam self-trapping to measure optical nonlinearities in planar waveguides. Beam self-trapping occurs when diffraction is counteracted by nonlinear index change induced by the beam itself [23]. Such an effect can even lead to the formation of a spatial soliton when the trapped beam propagates without changing its shape. The technique is used to characterize ultrafast nonlinear properties of three different selenide waveguides at 1550 and 1200 nm.

## 2. Beam self-trapping technique

It consists in focusing a pulsed laser at the input face of a slab waveguide while the beam profile is monitored with a camera at the output face. If the launched beam is narrow, typically few 10's of micron wide, it clearly enlarges due to diffraction in the linear regime along few millimeters propagation distance. In the nonlinear regime, i.e. at higher power, diffraction is modified due to either self-focusing or self-defocusing. To properly model the propagation, the effects of both linear and nonlinear absorption must be considered. The nonlinear Schrödinger equation that includes absorption can be written as [10]

$$\frac{\partial E(x, y, z)}{\partial z} - \frac{i}{2k} \frac{\partial^2 E(x, y, z)}{\partial x^2} + \frac{\alpha}{2} E(x, y, z) - i \frac{2\pi}{\lambda} n_2 I E(x, y, z) = 0. \quad (1)$$

Here,  $E(x, y, z)$  is the beam electric field distribution and is related to the beam intensity distribution by  $I = 1/2c\epsilon_0 n |E|^2$ .  $x$  and  $y$  are the coordinates parallel and perpendicular to the chalcogenide layer, respectively, and  $z$  is the coordinate associated to the propagation direction.  $n_2$  is the Kerr coefficient defined by  $n = n_0 + n_2 I$  where  $n_0$  is the effective linear refractive index of the guided mode,  $k = 2\pi n_0/\lambda$  is the propagation constant in the medium at the wavelength  $\lambda$ . The second term of Eq. (1) corresponds to diffraction that only occurs along  $x$  since the beam is guided along  $y$ -axis. The third term accounts for absorption  $\alpha$  expressed as  $\alpha = \alpha_1 + \alpha_2 I$ ,  $\alpha_1$  and  $\alpha_2$  being the linear and

TPA coefficients respectively. The contributions of three-photon and higher order absorption are neglected [24]. The last term of Eq. (1) accounts for the contribution of the Kerr nonlinearity. For a positive  $n_2$  coefficient and within certain power constraints, self-focusing effect can compensate for diffraction and the fundamental solution of Eq. (1) leads to a spatial soliton [25]. In our work, the Kerr coefficient will be deduced by fitting the experimental results with simulations given by the nonlinear Schrödinger Eq. (1) solved with a beam propagation method (BPM) [26].

## 3. Optical characterization of slab waveguides

The proposed technique is applied to characterize slab waveguides that consist of  $\text{Ge-Sb-Se}$  films deposited on top of a 500  $\mu\text{m}$  thick oxidized silicon substrate by radio frequency (RF) sputtering technique [27]. The deposition was carried out at a working pressure of  $5 \cdot 10^{-3}$  mbar. Three slab waveguides were fabricated by magnetron radio-frequency sputtering from three chalcogenide glass targets of the pseudo-binary system ( $\text{GeSe}_2\text{-Sb}_2\text{Se}_3$ ):  $\text{Ge}_{28.1}\text{Sb}_{6.3}\text{Se}_{65.6}$ ,  $\text{Ge}_{19.4}\text{Sb}_{16.7}\text{Se}_{63.9}$  and  $\text{Ge}_{12.5}\text{Sb}_{25}\text{Se}_{62.5}$ , later called Se2, Se4, and Se6. The characteristics of these selenide waveguides are summarized in Table 1. The chalcogenide guiding layer thickness of 3.0–3.2  $\mu\text{m}$  is determined by ellipsometry and scanning electron microscope techniques. The structure and physicochemical properties of the RF sputtered selenide films were analyzed using micro-Raman spectroscopy, Energy Dispersive X-ray Spectroscopy and X-ray Photoelectron Spectroscopy [28,29] and they are found to present some similarity to the bulk glass target prepared by the conventional melting and quenching technique depending on deposition conditions [21]. The material band gap energy from 1.70 to 2.11 eV was deduced by the variable angle spectroscopic ellipsometry method. The high refractive index of chalcogenide film and the presence of lower refractive index  $\text{SiO}_2$  layer form step index waveguides with high index contrast. Prism coupling technique is used to analyze the guiding properties. The slab waveguide is multimode at 1550 nm. The measured refractive index at 1550 nm is 2.93, 2.68, and 2.47 for respectively Se6, Se4, and Se2. By cleaving the crystalline silicon substrate, samples with high quality end faces are produced. Efficient light end-fire coupling into the waveguide is thus possible.

As shown in Fig. 1, the optical nonlinear measurements are performed with 200 fs laser pulses from a tunable optical parametric oscillator (OPO) with an 80 MHz repetition rate. The OPO is tuned to operate either at 1550 nm or 1200 nm. The laser beam is reshaped to an elliptical spot by a cylindrical lens and focused by a X40 microscope objective. The spot size at the entrance of the waveguide at a wavelength of 1.55  $\mu\text{m}$  is  $4 \times 33 \mu\text{m}$  (FWHM) in the guided ( $y$ ) and transverse dimension ( $x$ ), respectively. It is slightly smaller at 1200 nm in accordance with the wavelength dependence. The impact of the cumulative thermal effect is excluded with an optical chopper as it will be shown later. The sample is mounted on an  $XYZ$  translation stage to get the maximum light coupling. The spot size allows end fire coupling to the fundamental mode of the waveguide. A coupling efficiency of  $\sim 21\%$  is measured in our waveguides. The combination of a half-wave plate and a polarizer is used to vary the coupled power. Beam distribution at the output face of the chalcogenide film is monitored with a Vidicon camera using a X10 microscope objective while two calibrated power meters measure the input and output powers.

In order to accurately fit the experimental data with Eq. (1), we first determine the linear absorption and TPA of the waveguides. Cutback method is first used to measure the linear loss. The measurements are performed by cutting the waveguide into two different lengths, starting from the long propagation length  $z_2 = 1$  cm to a small length  $z_1 = 0.5$  cm. We make sure that the same power is coupled in both waveguides by optimizing the coupling efficiency. The following equation is then used to calculate the linear losses,

$$\alpha_1 = \frac{\ln\left(\frac{P_1}{P_2}\right)}{z_2 - z_1}, \text{ for } z_2 > z_1, \quad (2)$$

**Table 1**  
Material parameters for the chalcogenide thin films.

Sample	Theoretical composition	Guiding layer thickness ( $\mu\text{m}$ )	$E_g$ (eV)	Prism coupling technique $n_0$ (1550 nm)
Se6	$\text{Ge}_{12.5}\text{Sb}_{25}\text{Se}_{62.5}$	3.0	1.70	2.93
Se4	$\text{Ge}_{19.4}\text{Sb}_{16.7}\text{Se}_{63.9}$	3.0	1.86	2.68
Se2	$\text{Ge}_{28.1}\text{Sb}_{6.3}\text{Se}_{65.6}$	3.2	2.11	2.47

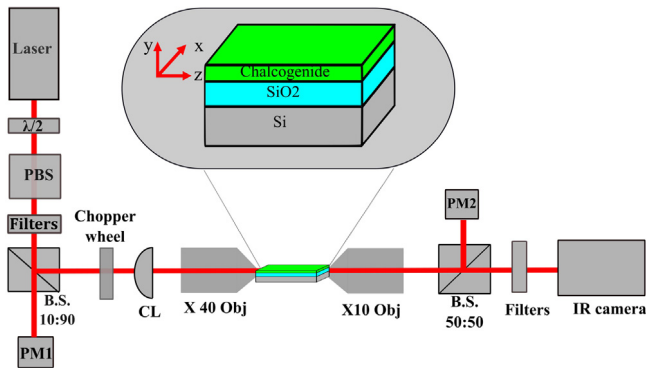


**Fig. 1.** Experimental setup used to analyze the beam self-action in chalcogenide planar waveguides.  $\lambda/2$ , half-wave plate; PBS, polarizing beam splitter; CL, cylindrical lens; Obj, microscope objective; PM, power meters; B.S, beam splitter.

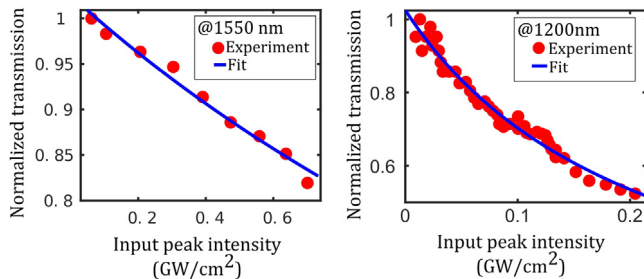


**Fig. 2.** The normalized transmission as a function of input intensity at 1550 nm and 1200 nm for 1 cm long Se4 sample; Red circles: experimental data, Blue lines: data fitting using Eq. (3).

where  $p_1$ ,  $p_2$  are the transmitted power for the short and long sample [30]. The linear absorption coefficient of waveguides, extracted from cut back method, is included in Table 2. Linear losses of  $0.19 \text{ cm}^{-1}$  for Se2,  $0.24 \text{ cm}^{-1}$  for Se4, and  $0.26 \text{ cm}^{-1}$  for Se6 are measured at 1550 nm. As expected, loss is decreasing as material bandgap energy increases. Since the photon energy is closer to the material bandgap at 1200 nm, larger propagation losses range from  $0.63 \text{ cm}^{-1}$  for Se2 to  $0.76 \text{ cm}^{-1}$  for Se6 are determined. Comparison with data found in the literature is not straightforward since ternary glasses of the very same composition have not been studied or different wavelengths have been considered. The propagation loss values measured in our three planar waveguides at 1200 nm are consistent with the waveguiding loss values measured at 1064 nm in the compositions of  $\text{Ge}_{29.9}\text{Sb}_{15.6}\text{Se}_{54.5}$  prepared by RF sputtering presenting a deficit in selenium [31]. At 1550 nm, the values can be compared to those found in corresponding bulk glasses of similar composition [21]. Our waveguides present larger losses (Table 2) than the values measured in bulk, which may be attributed to additional losses due to the waveguide imperfection.

To evaluate the TPA coefficients of the planar waveguides at both wavelengths, transmission versus launched optical power is recorded. The experimental setup (Fig. 1) designed for beam self-action analysis is slightly modified by introducing two power meters with the aid of beam splitters. The light power before and after the waveguide is thus monitored to deduce the transmission as a function of injected power. The measurements are repeated several times at different positions in the sample to minimize experimental error. Fresnel losses at the input

of the waveguide are considered to deduce the input peak intensity. The nonlinear absorption coefficient  $\alpha_2$  is then deduced by fitting the experimental data with the following equation which gives the normalized transmission as a function of input peak intensity  $I_0$  [32]

$$\frac{T}{T_{\max}} = \frac{1}{\frac{1}{\alpha_1} [\alpha_1 + \alpha_2 I_0 (1 - \exp(-\alpha_1 l))]} \quad (3)$$

where  $T_{\max}$  is the transmission at low input peak intensity and  $l$  is the sample length. Fig. 2 represents typical transmission curves as a function of input intensity in a 1 cm long Se4 sample at 1550 nm and 1200 nm wavelengths. The fitting coefficients  $\alpha_2$  obtained for the different waveguides are given in Table 2. We observe that the TPA coefficients do not vary monotonically versus material bandgap energy. In our samples, the largest TPA coefficients are measured at 1200 nm and increase with decreasing material bandgap energy. However, measurement uncertainty is too large to conclude. It is however important to note that the values estimated for compositions similar to Se4 and Se2 by Petit et al. [33] at 1064 nm are in good agreement with the values we found at 1200 nm. They have demonstrated that the  $\alpha_2$  varies from  $(1.6 \pm 0.2) \text{ cm} \cdot \text{GW}^{-1}$  to  $(4.9 \pm 0.6) \text{ cm} \cdot \text{GW}^{-1}$  depending upon the Ge–Sb–Se composition. TPA is weak at 1550 nm in Se2 and Se4 with values consistent with measurements performed in bulk samples of similar composition by transmission analysis [21] and by Wang et al. by open aperture Z-scan [18] given in Table 2. The values obtained from the best fits range from  $0.37 \text{ cm/GW}$  (Se4 at 1550 nm) to  $5.5 \text{ cm/GW}$  (Se6 at 1200 nm) and increases with incident photon energy. These values are approximately 3 times smaller than the TPA value measured in selenide strip waveguides at 1030 nm with 7 ps pulses by an Yb-doped fiber laser [22].

While previous measurements are standard, the originality of our method to determine the  $n_2$  coefficient is based on the beam self-action analysis. A typical observation made in a 1 cm long Se6 slab waveguide at 1550 nm is depicted in Fig. 3. Fig. 3(a) shows the shape of the beam at the entrance of the waveguide whose horizontal size is  $33 \mu\text{m}$  FWHM. At low incident intensity, the beam propagates in linear regime and diffracts freely to give an output beam whose FWHM is about  $78 \mu\text{m}$  (Fig. 3(b)). As we increase the input peak intensity, we observe a beam narrowing which reveals a positive  $n_2$  coefficient. Adjustment of the beam input peak intensity to  $0.30 \text{ GW/cm}^2$  even leads to the formation of a trapped beam close to a spatial soliton as depicted in Fig. 3(c). Formation of Kerr spatial soliton is confirmed when the input and output beam profiles are similar. In such a situation, diffraction and self-focusing compensates each other.

Since our measurements are made with a high repetition rate laser (80 MHz), it is important to evaluate the contribution of potential thermal effect or photo-induced effects that could be present in addition to the instantaneous electronic nonlinearity. Following the literature [37–39], we performed experiments with an optical chopper in order to lower the average power while maintaining the peak power. A chopping frequency of 1000 Hz and a duty cycle of 28% was used. Fig. 4 depicts the self-focusing behavior versus intensity in the Se6 sample with and without the chopper at both 1550 nm and 1200 nm. Note that the Se6 composition has the lowest bandgap energy and consequently the strongest absorption which would favor appearance of the thermal effect. Within the experimental errors, no change in FWHM beam behavior is observed despite an average power divided by more than 3.5 times with the chopper compared to without chopper. It clearly demonstrates that thermal effect can be neglected in these glasses when working at near infrared wavelengths with femtosecond laser

**Table 2**

Measured values of the optical coefficients in the three chalcogenide waveguides at 1550 nm and 1200 nm. To validate the measurements, optical coefficients of the chalcogenide glasses/waveguides obtained by other techniques are presented (BSA, beam self-trapping analysis; DTA, direct transmission analysis; SRTBC, spectrally resolved two beam coupling).

Sample	$\lambda$ (nm)	$\alpha_1$ (cm <sup>-1</sup> )	$\alpha_2$ (cm · GW <sup>-1</sup> )	$n_2$ (10 <sup>-18</sup> m <sup>2</sup> · W <sup>-1</sup> )	Method & References
Se6/ Ge <sub>12.5</sub> Sb <sub>25</sub> Se <sub>62.5</sub>					
Slab waveguide	1550	0.26	1.66 ± 0.18	35 ± 10	BSA
Slab waveguide	1200	0.76	5.5 ± 0.8	69 ± 11	BSA
Bulk	1550	0.2	0.84	20.3 ± 3	DTA [21]
Se4/ Ge <sub>19.4</sub> Sb <sub>16.7</sub> Se <sub>63.9</sub>					
Slab waveguide	1550	0.24	0.37 ± 0.05	15 ± 4	BSA
Slab waveguide	1200	0.71	5.4 ± 0.6	50 ± 12	BSA
Bulk	1550	0.15	0.31	9.97 ± 2	DTA [21]
Se2/Ge <sub>28.1</sub> Sb <sub>6.3</sub> Se <sub>65.6</sub>					
Slab waveguide	1550	0.19	0.43 ± 0.06	9 ± 1	BSA
Slab waveguide	1200	0.63	2.7 ± 0.4	36 ± 11	BSA
Bulk	1550	0.15	0.29	9.0 ± 2	DTA [21]
Ge <sub>29.9</sub> Sb <sub>15.6</sub> Se <sub>54.5</sub> (waveguide)	1064	0.806–0.852			[31]
Ge <sub>23</sub> Sb <sub>7</sub> Se <sub>70</sub> (bulk)	1064		2.4		Z-scan [33]
Ge <sub>28</sub> Sb <sub>7</sub> Se <sub>65</sub> (bulk)	1064		4.9 ± 0.6		Z-scan [33]
Ge <sub>23</sub> Sb <sub>7</sub> S <sub>70</sub> (ridge waveguide)	1550			3.71	SPM [34]
Ge–Sb–Se (bulk)	1150–1686		0.05–7.44	7.33–20.3	Z-scan [18]
As <sub>2</sub> Se <sub>3</sub> (bulk)	1500			19	Z-scan [35]
	1250		2.8 ± 0.4	30 ± 4.5	SRTBC [36]
As <sub>2</sub> S <sub>3</sub> (bulk)	1250		0.16 ± 0.02	6.8 ± 1.0	SRTBC [36]

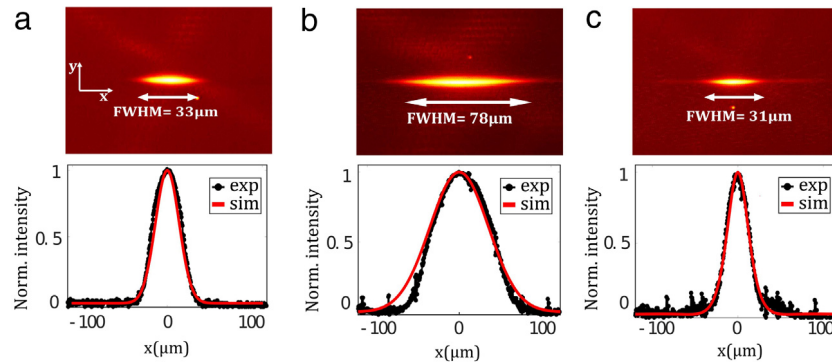


**Fig. 3.** Experimental images and comparison between experimental and numerical beam profiles of beam self-action analysis as a function of input peak intensity within a 1 cm long Se6 planar waveguide. Input beam injected into the waveguide (a), diffracted output beam in linear regime (b), output self-trapped beam near soliton propagation with a peak intensity of 0.30 GW/cm<sup>2</sup>(c). Circles and solid line profiles correspond to experimental and numerical fits, respectively.

system. Furthermore, we have also verified that the self-focusing effect is reversible when we switched from high intensity to low intensity. It proves that no permanent modification of refractive index that could be due to the glass photosensitivity [40] is induced during the experiment.

The experimental Kerr self-action regime should thus be modeled using Eq. (1) to deduce the  $n_2$  coefficient. Accuracy is however higher when the nonlinear regime reveals an obvious change in the experimental output profile. In the Se6 sample, soliton regime can be reached. We thus chose to consider this experimental regime for the fitting using the numerical simulations given by Eq. (1). The  $n_2$  coefficient being the only free variable while absorption coefficients are taken from the previous section. More precisely, we look for the  $n_2$  coefficient that predicts the experimental results numerically by the BPM method. A Gaussian input beam profile of identical width and same peak intensity as the experimental one is considered at the input of the numerical simulation. For instance, the solid line in Fig. 3(a), (b) shows the fitted beam profile in linear regime, respectively at the entrance and at the exit face of the 1 cm long Se6 sample at 1550 nm. Fig. 3(c) depicts the output beam profile in soliton regime for an input peak intensity  $I_0 = 0.30$  GW/cm<sup>2</sup>,  $\alpha_2 = 1.66$  cm · GW<sup>-1</sup>,  $\alpha_1 = 0.26$  cm<sup>-1</sup>, and  $n_2 = 35 \times 10^{-18}$  m<sup>2</sup> · W<sup>-1</sup>. The numerical simulation results give a beam FWHM of 31.5 μm, 79 μm and 31.5 μm respectively for input beam, diffracted output beam in linear regime and soliton beam profiles, which are in good agreement with the experimental beam profiles as shown in Fig. 3. Further increase

of intensity leads to the formation of side wings and beam breakup. This could be explained by considering the contribution of TPA at high intensity [41,42]. Moreover, waveguide facet damage occurs when the excitation intensity exceeds 0.82 GW/cm<sup>2</sup> for Se6 samples at 1550 nm. Two experimental parameters lead to some uncertainty in the evaluation of  $n_2$ , the input beam FWHM and the input beam intensity. The beam width uncertainty is about 2 μm while the uncertainty of the incident intensity is evaluated to be 10%. So, we first deduced  $n_2$  corresponding to soliton formation intensity with the parameters of input beam FWHM,  $n_0$ ,  $\lambda$ ,  $\alpha_1$  and  $\alpha_2$ . Then we calculated  $n_2$  coefficients for an input peak intensity, which is 10% above and below the soliton intensity. Fig. 5 shows the calculated the beam FWHM at the exit face of a 1 cm long waveguide as a function of  $n_2$  coefficient for two different incident intensities. Dependence of the expected FWHM versus  $n_2$  is found to be linear. The estimated uncertainty on intensity dependent  $n_2$  is 28.5% for Se6.

Similar experiments have been performed in Se4 and Se2 samples at 1550 nm and 1200 nm. Fig. 6 presents the evolution of the output beam FWHM as a function of the input peak intensity for the three waveguides at 1550 nm. Since they are all about 1 cm long, diffraction regimes are similar. At low incident intensity, output beam diffracts to give a beam, which is 2.4 times larger than the input beam. For all samples, self-trapping is observed ( $n_2 > 0$ ) and soliton formations can be reached. Soliton is formed at input peak intensities of 0.30 GW/cm<sup>2</sup> for Se6, 0.95

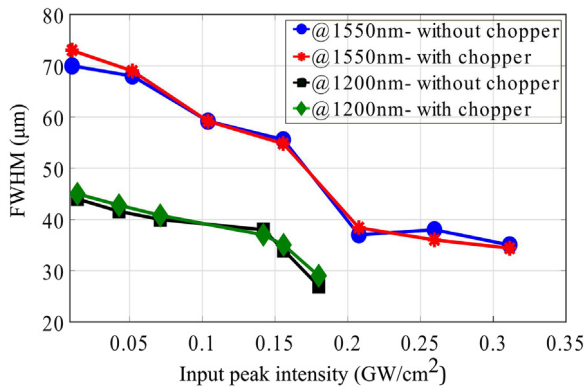


Fig. 4. Evolution of output beam FWHM as a function of intensity in Se6 at 1550 and 1200 nm with and without optical chopper.

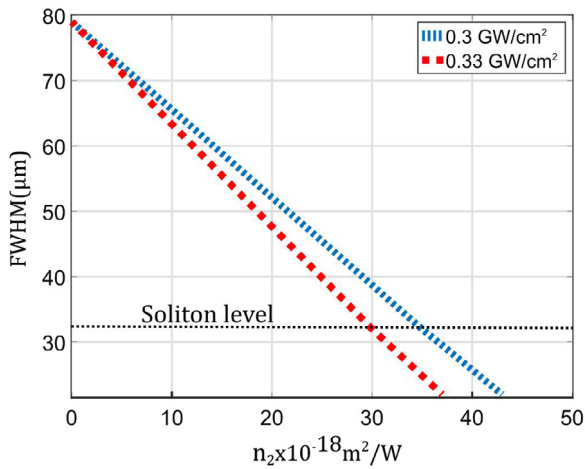


Fig. 5. Computed output beam FWHM versus nonlinear refractive index  $n_2$  in Se6 chalcogenide waveguide. Parameters: Input beam FWHM = 33  $\mu\text{m}$ , linear refractive index = 2.93,  $\lambda = 1550 \text{ nm}$ ,  $\alpha_1 = 0.26 \text{ cm}^{-1}$ ,  $\alpha_2 = 1.66 \text{ cm/GW}$ , waveguide length = 1 cm.

GW/cm<sup>2</sup> for Se4 and 1.28 GW/cm<sup>2</sup> for Se2, respectively. Note that to prevent input facet damage we voluntarily did not go beyond the soliton power in the tested samples. We have also confirmed the absence of thermal or photosensitivity effect in Se4 and Se2 samples. The same technique is used to characterize the nonlinear properties at 1200 nm. Strong self-trapping and formation of spatial soliton are observed in the three waveguides at 1200 nm, but with lower input intensity than 1550 nm. Table 2 summarizes the results of optical constant measurements for the three studied planar chalcogenide waveguides at the two different wavelengths. The measurements showed that both  $n_2$  and TPA are smaller in Se2 in accordance with its larger band gap than Se4 and Se6.

To validate our method, we compare our values with the ones obtained by other techniques. The experimental  $n_2$  values obtained for Se4 and Se2 waveguides by the beam self-trapping analysis at 1550 nm are close to the values obtained in bulk samples of similar composition (See Table 2) characterized by the Z-scan techniques [21]. In addition, our  $n_2$  values measured for Se4 and Se2 are consistent with the values reported by Dai et al. in Ge–Sb–Se ternary system using the Z-scan technique in femtosecond regime [19]. They estimated values of  $n_2$  vary from  $5.3 \times 10^{-18} \text{ m}^2/\text{W}$  to  $19 \times 10^{-18} \text{ m}^2/\text{W}$  at 1550 nm for different compositions of Ge–Sb–Se glasses. A recent paper [34] reported the nonlinear characterization of a Ge<sub>23</sub>Sb<sub>7</sub>S<sub>70</sub> ridge waveguide using the self-phase modulation to be  $3.71 \times 10^{-18} \text{ m}^2/\text{W}$  at the wavelength of 1550 nm. In Ge–Sb–Se samples, we obtained  $n_2$  as high as  $(35 \pm 10) \times 10^{-18} \text{ m}^2/\text{W}$  at 1550 nm and  $(69 \pm 11) \times 10^{-18} \text{ m}^2/\text{W}$  at 1200 nm for the sample

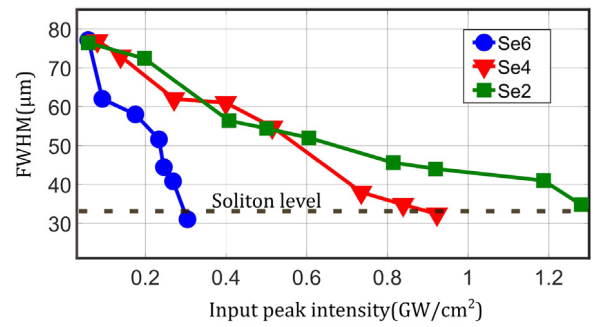


Fig. 6. Measured output beam FWHM as a function of input peak intensity in the three-selenide compositions at 1550 nm.

with the smallest bandgap. This is in accordance with a nonlinearity four times larger in As<sub>2</sub>Se<sub>3</sub> than in As<sub>2</sub>S<sub>3</sub> [35,36]. This clearly reveals that  $n_2$  increases as selenium is substituted for sulfur atoms. Moreover,  $n_2$  increases as material bandgap decreases. This trend is consistent with values reported by Wang et al. where the wavelength was tuned from 1150 nm to 1686 nm [18]. It is also important to note that some properties of the bulk materials such as the chemical composition, the band gap energy, and the refractive index are known to slightly differ from properties of deposited films [43]. The sputtered films fabricated with low Ar pressure present a deficit of selenium of about 2–3%. Consequently, nonlinear optical properties of bulk target and deposited films do not exactly match. Nonetheless, the intensity dependent  $n_2$  values measured by the beam self-trapping analysis follows the same trends than the one estimated by the Z-scan method in Ge–Sb–Se glasses. All results validate our original technique.

In conclusion, we have shown that beam profile analysis due to beam self-trapping is an accurate and simple technique to deduce optical Kerr effect in planar waveguides. This technique has been applied to measure ultrafast optical properties in three slab waveguides of Ge<sub>28.1</sub>Sb<sub>6.3</sub>Se<sub>65.6</sub>, Ge<sub>19.4</sub>Sb<sub>16.7</sub>Se<sub>63.9</sub> and Ge<sub>12.5</sub>Sb<sub>25</sub>Se<sub>62.5</sub> composition at the wavelength of 1550 and 1200 nm. The deduced  $n_2$  values are consistent with measurements performed with different techniques in bulk samples of similar composition. A Kerr nonlinearity as high as  $(69 \pm 11) \times 10^{-18} \text{ m}^2 \cdot \text{W}^{-1}$  is found at 1200 nm in Ge<sub>12.5</sub>Sb<sub>25</sub>Se<sub>62.5</sub> films. The strong ultrafast nonlinearities together with Kerr spatial soliton formation and low propagation losses of the Ge–Sb–Se fabricated planar waveguides make them suitable for nonlinear photonic devices such as wavelength conversion or super continuum generation.

### Acknowledgments

The authors are grateful for the financial support of the Region Franche-Comté. This work was partly supported by the RENATECH network and its FEMTO-ST MIMENTO technological facility.

### References

- [1] M. Asobe, K. Suzuki, T. Kanamori, K. Kubodera, Nonlinear refractive index measurement in chalcogenide-glass fibers by self-phase modulation, *Appl. Phys. Lett.* 60 (1992) 1153–1154.
- [2] G. Boudebs, M. Chis, X.N. Phu, Third-order susceptibility measurement by a new Mach-Zehnder interferometry technique, *JOSA B.* 18 (2001) 623–627.
- [3] H. Kanbara, S. Fujiwara, K. Tanaka, H. Nasu, K. Hirao, Third-order nonlinear optical properties of chalcogenide glasses, *Appl. Phys. Lett.* 70 (1997) 925–927.
- [4] K. Tanaka, Two-photon absorption spectroscopy of As<sub>2</sub>S<sub>3</sub> glass, *Appl. Phys. Lett.* 80 (2002) 177–179.
- [5] M. Asobe, T. Kanamori, K. Kubodera, Ultrafast all-optical switching using highly nonlinear chalcogenide glass fiber, *IEEE Photon. Technol. Lett.* 4 (1992) 362–365.
- [6] M. Sheik-Bahae, A.A. Said, T.-H. Wei, D.J. Hagan, E.W. Van Stryland, Sensitive measurement of optical nonlinearities using a single beam, *IEEE J. Quantum Electron.* 26 (1990) 760–769.

- [7] Z.H. Zhou, T. Hashimoto, H. Nasu, K. Kamiya, Two-photon absorption and nonlinear refraction of lanthanum sulfide-gallium sulfide glasses, *J. Appl. Phys.* 84 (1998) 2380–2384.
- [8] B.J. Eggleton, B. Luther-Davies, K. Richardson, Chalcogenide photonics, *Nature Photon.* 5 (2011) 141–148.
- [9] J. Leuthold, C. Koos, W. Freude, Nonlinear silicon photonics, *Nat. Photon.* 4 (2010) 535–544.
- [10] J.S. Aitchison, D.C. Hutchings, J.U. Kang, G.I. Stegeman, A. Villeneuve, The nonlinear optical properties of algaas at the half band gap, *IEEE J. Quantum Electron.* 33 (1997) 341–348.
- [11] V. Coda, R.D. Swain, H. Maillotte, G.J. Salamo, M. Chauvet, Wavelength, power and pulse duration influence on spatial soliton formation in AlGaAs, *Opt. Commun.* 251 (2005) 186–193.
- [12] A.M. Bagrov, P.I. Baikalov, A.V. Vasil'ev, G.G. Devyatkykh, E.M. Dianov, V.G. Plotnichenko, I.V. Skripachev, V.K. Sysoev, M.F. Churbanov, Fiber waveguides for the middle infrared range made of As–S and As–Se glasses with optical losses below 1 dB/m, *Sov. J. Quantum Electron.* 13 (1983) 1264.
- [13] J.T. Gopinath, M. Soljačić, E.P. Ippen, V.N. Puflyigin, W.A. King, M. Shurgalin, Third order nonlinearities in Ge–As–Se-based glasses for telecommunications applications, *J. Appl. Phys.* 96 (2004) 6931–6933.
- [14] M. Chauvet, G. Fanjoux, K.P. Huy, V. Nazabal, F. Charpentier, T. Billeton, G. Boudebs, M. Cathelinaud, S.-P. Gorza, Kerr spatial solitons in chalcogenide waveguides, *Opt. Lett.* 34 (2009) 1804–1806.
- [15] L. Petit, N. Carlie, F. Adamietz, M. Couzi, V. Rodriguez, K.C. Richardson, Correlation between physical, optical and structural properties of sulfide glasses in the system Ge–Sb–S, *Mater. Chem. Phys.* 97 (2006) 64–70.
- [16] M. Olivier, P. Němec, G. Boudebs, R. Boidin, C. Focsa, V. Nazabal, Photosensitivity of pulsed laser deposited Ge–Sb–Se thin films, *Opt. Mater. Express.* 5 (2015) 781.
- [17] L. Chen, F. Chen, S. Dai, G. Tao, L. Yan, X. Shen, H. Ma, X. Zhang, Y. Xu, Third-order nonlinearity in Ge–Sb–Se glasses at mid-infrared wavelengths, *Mater. Res. Bull.* 70 (2015) 204–208.
- [18] T. Wang, X. Gai, W. Wei, R. Wang, Z. Yang, X. Shen, S. Madden, B. Luther-Davies, Systematic z-scan measurements of the third order nonlinearity of chalcogenide glasses, *Opt. Mater. Express.* 4 (2014) 1011.
- [19] S. Dai, F. Chen, Y. Xu, Z. Xu, X. Shen, T. Xu, R. Wang, W. Ji, Mid-infrared optical nonlinearities of chalcogenide glasses in Ge–Sb–Se ternary system, *Opt. Express* 23 (2015) 1300.
- [20] P. Němec, M. Olivier, E. Baudet, A. Kalendová, P. Benda, V. Nazabal, Optical properties of  $(\text{GeSe}_2)_{100-x}(\text{Sb}_2\text{Se}_3)_x$  glasses in near- and middle-infrared spectral regions, *Mater. Res. Bull.* 51 (2014) 176–179.
- [21] M. Olivier, J.C. Tchahame, P. Němec, M. Chauvet, V. Besse, C. Cassagne, G. Boudebs, G. Renversez, R. Boidin, E. Baudet, V. Nazabal, Structure, nonlinear properties, and photosensitivity of  $(\text{GeSe}_2)_{100-x}(\text{Sb}_2\text{Se}_3)_x$  glasses, *Opt. Mater. Express.* 4 (2014) 525.
- [22] M.R. Krogstad, S. Ahn, W. Park, J.T. Gopinath, Nonlinear characterization of  $\text{Ge}_{28}\text{Sb}_{12}\text{Se}_{60}$  bulk and waveguide devices, *Opt. Express* 23 (2015) 7870.
- [23] R.Y. Chiao, E. Garmire, C.H. Townes, Self-trapping of optical beams, *Phys. Rev. Lett.* 13 (1964) 479.
- [24] A. Zakery, S.R. Elliott, *Optical Nonlinearities in Chalcogenide Glasses and their Applications*, Springer, New York, 2007.
- [25] S. Trillo, W. Torruellas, *Spatial Solitons*, Springer, New York, 2001.
- [26] L. Thylen, The beam propagation method: an analysis of its applicability, *Opt. Quantum Electron.* 15 (1983) 433–439.
- [27] V. Nazabal, F. Charpentier, J.-L. Adam, P. Nemeč, H. Lhermite, M.-L. Brandily-Anne, J. Charrier, J.-P. Guin, A. Moréac, Sputtering and pulsed laser deposition for near- and mid-infrared applications: A comparative study of  $\text{Ge}_{25}\text{Sb}_{10}\text{Se}_{65}$  and  $\text{Ge}_{25}\text{Sb}_{10}\text{Se}_{65}$  amorphous thin films: Sputtering and pulsed laser deposition for near- and mid-IR applications, *Int. J. Appl. Ceram. Technol.* 8 (2011) 990–1000.
- [28] E. Baudet, A. Gutierrez-Arroyo, P. Němec, L. Bodiou, J. Lemaitre, O. De Sagazan, H. Lhermitte, E. Rinnert, K. Michel, B. Bureau, J. Charrier, V. Nazabal, Selenide sputtered films development for MIR environmental sensor, *Opt. Mater. Express.* 6 (2016) 2616.
- [29] E. Baudet, C. Cardinaud, A. Girard, E. Rinnert, K. Michel, B. Bureau, V. Nazabal, Structural analysis of RF sputtered Ge–Sb–Se thin films by Raman and X-ray photoelectron spectroscopies, *J. Non-Cryst. Solids* 444 (2016) 64–72.
- [30] R.D. Driver, G.M. Leskowitz, L.E. Curtiss, D.E. Moynihan, L.B. Vacha, The characterization of infrared transmitting optical fibers, in: *MRS Proc*, Cambridge Univ Press, 1989, p. 169.
- [31] R.K. Watts, M. de Wit, W.C. Holton, Nonoxide chalcogenide glass films for integrated optics, *Appl. Opt.* 13 (1974) 2329–2332.
- [32] J.S. Aitchison, Y. Silberberg, A.M. Weiner, D.E. Leaird, M.K. Oliver, J.L. Jackel, E.M. Vogel, P.W.E. Smith, Spatial optical solitons in planar glass waveguides, *JOSA B* 8 (1991) 1290–1297.
- [33] L. Petit, N. Carlie, H. Chen, S. Gaylord, J. Massera, G. Boudebs, J. Hu, A. Agarwal, L. Kimerling, K. Richardson, Compositional dependence of the nonlinear refractive index of new germanium-based chalcogenide glasses, *J. Solid State Chem.* 182 (2009) 2756–2761.
- [34] J.W. Choi, Z. Han, B.-U. Sohn, G.F.R. Chen, C. Smith, L.C. Kimerling, K.A. Richardson, A.M. Agarwal, D.T.H. Tan, Nonlinear characterization of GeSbS chalcogenide glass waveguides, *Sci. Rep.* 6 (2016) 39234.
- [35] G. Lenz, J. Zimmermann, T. Katsufuji, M.E. Lines, H.Y. Hwang, S. Spälter, R.E. Slusher, S.-W. Cheong, J.S. Sanghera, Id. Aggarwal, Large Kerr effect in bulk Se-based chalcogenide glasses, *Opt. Lett.* 25 (2000) 254–256.
- [36] J.M. Harbold, F.Ö. Ilday, F.W. Wise, J.S. Sanghera, V.Q. Nguyen, L.B. Shaw, I.D. Aggarwal, Highly nonlinear As–S–Se glasses for all-optical switching, *Opt. Lett.* 27 (2002) 119–121.
- [37] M. Falconieri, G. Salvetti, Simultaneous measurement of pure-optical and thermo-optical nonlinearities induced by high-repetition-rate, femtosecond laser pulses: application to CS<sub>2</sub>, *Appl. Phys. B Lasers Opt.* 69 (1999) 133–136.
- [38] P. Burkins, R. Kuis, I. Basaldua, A.M. Johnson, S.R. Swaminathan, D. Zhang, S. Trivedi, Thermally managed Z-scan methods investigation of the size-dependent nonlinearity of graphene oxide in various solvents, *J. Opt. Soc. Amer. B* 33 (2016) 2395.
- [39] A. Gnoli, L. Razzari, M. Righini, Z-scan measurements using high repetition rate lasers: how to manage thermal effects, *Opt. Lett.* 20 (2005) 7976–7981.
- [40] A.E. Owen, A.P. Firth, P.J.S. Ewen, Photo-induced structural and physico-chemical changes in amorphous chalcogenide semiconductors, *Philos. Mag. B* 52 (1985) 347–362.
- [41] Y. Silberberg, Solitons and two-photon absorption, *Opt. Lett.* 15 (1990) 1005–1007.
- [42] N.N. Akhmediev, A. Ankiewicz, *Solitons, Nonlinear Pulses and Beams*, Chapman & Hall, London, 1997.
- [43] E. Baudet, M. Sergent, P. Němec, C. Cardinaud, E. Rinnert, K. Michel, L. Jouany, B. Bureau, V. Nazabal, Experimental design approach for deposition optimization of RF sputtered chalcogenide thin films devoted to environmental optical sensors, *Sci. Rep.* 7 (2017) 3500.